J Paleolimnol (2011) 45:85–99
DOI 10.1007/s10933-010-9482-9

ORIGINAL PAPER

Middle to late Holocene initiation of the annual flood pulse in Tonle Sap Lake, Cambodia

Mary Beth Day · David A. Hodell · Mark Brenner · Jason H. Curtis · George D. Kamenov · Thomas P. Guilderson · Larry C. Peterson · William F. Kenney · Alan L. Kolata

Received: 25 February 2010 / Accepted: 28 October 2010 / Published online: 25 November 2010

Abstract Tonle Sap Lake, Cambodia, possesses one of the most productive inland fisheries in the world and is a vital natural resource for the country. The lake is connected to the Mekong River via the Tonle Sap River. Flow in the Tonle Sap River reverses seasonally, with water exiting the lake in the dry season and entering the lake during the summer monsoon. This flood pulse drives the lake's biological productivity. We used Sr, Nd, and Pb isotopes and elemental concentrations in lake sediment cores to track changes in the provenance of deposits in Tonle Sap Lake. We sought to determine when the lake first began to receive water and sediment input via the Mekong River, which initiated flood pulse processes. The transition from a non-pulsing lake to the Mekong-connected system is marked by shifts to values of $^{87}Sr/^{86}Sr$, ε_{Nd}, and $^{207}Pb/^{204}Pb$ that are characteristic of Mekong River sediments. In addition, magnetic susceptibility increased and sediment elemental composition changed. Elemental (P) measures point to enhanced phosphorus loading and C/N and isotope ratios of bulk organic matter indicate a shift to greater relative contribution of organic material from aquatic versus terrestrial environments, coinciding with the initiation of flood pulse processes. On the basis of radiocarbon dating in two cores, we estimate the initiation of the annual flood pulse occurred between ~4,450 and 3,910 cal year BP.

Electronic supplementary material The online version of this article (doi:10.1007/s10933-010-9482-9) contains supplementary material, which is available to authorized users.

M. B. Day · J. H. Curtis · G. D. Kamenov
Department of Geological Sciences, University of Florida, Gainesville, FL 32611-2120, USA

D. A. Hodell
Godwin Laboratory for Palaeoclimate Research, Department of Earth Sciences, University of Cambridge, Cambridge CB2 3EQ, UK

M. Brenner · W. F. Kenney
Department of Geological Sciences and Land Use and Environmental Change Institute, University of Florida, Gainesville, FL 32611-2120, USA

T. P. Guilderson
Center for Accelerator Mass Spectrometry, Lawrence Livermore National Laboratory, Livermore, CA, USA

L. C. Peterson
Rosenstiel School of Marine and Atmospheric Science, University of Miami, Miami, FL, USA

A. L. Kolata
Department of Anthropology, University of Chicago, Chicago, IL, USA

Present Address:
M. B. Day (✉)
Department of Earth Sciences, University of Cambridge, Cambridge CB2 3EQ, UK
e-mail: mbd33@cam.ac.uk

Keywords Tonle Sap Lake · Flood pulse · Mekong River · Cambodia · Radiogenic isotopes

Introduction

Tonle Sap Lake, the largest freshwater body in Southeast Asia, is part of the Mekong River Basin. The Tonle Sap River joins the lake with the Mekong River (Fig. 1). During the dry season (November to April), water flows from the lake, through the Tonle Sap River, into the Mekong, and ultimately to the South China Sea. During the rainy months of the summer monsoon (May to October), however, an increase in hydraulic head at the confluence of the Mekong and Tonle Sap Rivers leads to a reversal of flow through the Tonle Sap River that allows Mekong floodwaters to enter Tonle Sap Lake. This annual flood pulse creates pronounced seasonal variability in lake morphometry. During the monsoon, mean depth increases from dry season values of 1–2 m to >10 m at maximum flood stage, and the lake's area grows approximately five-fold, from 2,500 to 3,000 km^2 to >15,000 km^2 (Baran 2005). Tonle Sap is essentially flat-bottomed, thus water depth is uniform throughout most of the permanently flooded portion of the lake basin.

The Tonle Sap-Mekong system is one of the most productive freshwater fisheries in the world, and fish from Tonle Sap provide the majority of the protein in the Cambodian diet (Baran 2005; Hortle et al. 2004). The lake's biological productivity is primarily the result of the annual flood pulse. Flood pulse systems are known to be highly productive (Junk and Wantzen 2004; Junk et al. 1989; Wantzen et al. 2008). The flood pulse concept (FPC) was first developed by Junk et al. (1989) to describe the relationships between the biotic and abiotic components of large river-floodplain systems and emphasized the exchange and recycling of nutrients and organic matter between the floodplain and the main river channel. The FPC has since been expanded to apply to lacustrine systems as well as rivers (Wantzen et al. 2008). Nutrients that support high levels of productivity in flood pulse systems are derived from the dissolved and suspended components of the floodwaters themselves, as well as the breakdown of organic matter in the floodplain, where alternation between aquatic and terrestrial conditions enhances decomposition (Junk et al. 1989). The relative contribution of imported versus recycled nutrients varies from system to system (Junk et al. 1989). The "flood pulse advantage" refers to the high fish yields generated by pulsing systems, in which fish take advantage of floodplain resources unavailable to fish in non-pulsing systems (Bayley 1991).

The Mekong River-derived flood pulse is the driving force of productivity in Tonle Sap Lake (Kummu and Sarkkula 2008; Lamberts 2001, 2008;

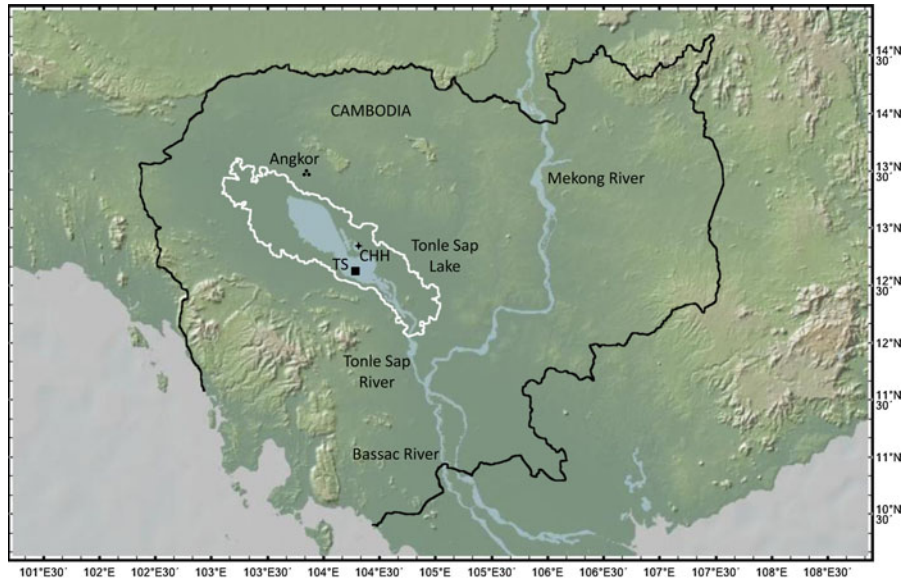

Fig. 1 Map of Cambodia. Both the permanently flooded and seasonally inundated portions of Tonle Sap Lake are shown. Core TS-18-XII-03 location denoted by a *square* and core CHH-17-XII-03 by a *cross*. Map created in GeoMapApp with GMRT (Ryan et al. 2009) and SRTM (Farr et al. 2007) data sets

Lamberts and Koponen 2008; MRCS/WUP-FIN 2003; Sarkkula et al. 2004). Hydrologic and productivity models of the Tonle Sap ecosystem indicate that fishery productivity is maximized by the following flood pulse-related conditions: (1) early arrival of floodwaters and long duration of flooding, (2) adequate flow to transport larvae and juvenile fish from the Tonle Sap River into Tonle Sap Lake, (3) a high flood level that inundates a large area, (4) maintenance of the plants that live in the inundated regions to ensure continued transfer of nutrients, and (5) continued input and utilization of sediments and nutrients carried by the floodwaters into the lake (Sarkkula et al. 2004).

Anthropogenic modification of Mekong River flow patterns through redirection of water for irrigation, and especially damming, has the potential to affect many aspects of the Tonle Sap flood pulse (Lamberts 2008). If flow through the Mekong becomes highly regulated, flooding will be minimized. This means the amplitude of the flood pulse will be diminished, and a smaller area will be inundated. The duration of flooding will also be reduced, and larvae and young fish may not be transported into the lake. Biogeochemical processes within the lake will be altered and this will affect water quality and nutrient dynamics. Furthermore, the sediment load will likely decrease as dams trap materials upstream. Sediments may be an important source of nutrients to floodplain soils as well as for lacustrine primary producers (MRCS/WUP-FIN 2003; Keskinen et al. 2005).

Given that biological productivity in Tonle Sap Lake is intrinsically linked to the annual flood pulse, an understanding of the system's historical hydrology is important for successful management of this natural resource. This study addresses two fundamental questions related to the paleoenvironmental history of Tonle Sap Lake and its flood pulse. First, when did Tonle Sap first begin to receive water and sediment input from the Mekong River? Second, how did the lake ecosystem respond to the initiation of the annual flood pulse? Radiogenic isotopes (Sr, Nd, Pb) were used to identify changes in sediment source attributed to the introduction of Mekong River sediments to the lake. C and N stable isotopes, C/N ratios, and phosphorus (P) concentrations were used to gauge the ecological response of Tonle Sap Lake to the initiation of the flood pulse.

Previous paleolimnological studies on Tonle Sap Lake

The paleoenvironmental history of Tonle Sap Lake was first investigated in the early 1960s (Carbonnel 1963; Carbonnel and Guiscafré 1965). Nineteen sediment cores were collected from the lake and analyzed for physical and chemical properties, including grain size, water content, iron content, and mineralogy (Carbonnel and Guiscafré 1965). Two sedimentary facies were identified, a "recent mud" that Carbonnel (1963) attributes to deposition under modern conditions, and an "ancient mud" that accumulated under significantly different environmental conditions. A piece of wood found near the bottom of the upper lithologic unit (recent mud) in one of the cores was dated to 5,720 ± 300 ^{14}C year BP (ESM 1). This transition from "ancient" to "modern" was attributed to the middle Holocene sea level maximum rather than hydrologic changes related to the Mekong River or the flood pulse (Carbonnel 1963; Carbonnel and Guiscafré 1965).

A later study examined the clay mineralogy of sediments from the Tonle Sap basin and proposed that the Mekong River became linked to Tonle Sap around 5,000 ^{14}C years BP (Okawara and Tsukawaki 2002). The same lithologic change observed by Carbonnel (1963) was noted in the core analyzed by Okawara and Tsukawaki (2002). Below the transition, the only clay minerals found were kaolinite and smectite, whereas above the transition, illite and chlorite were also present. Surface sediments from the Siem Reap River, a small input tributary to the lake, and soils from the alluvial plain near the north shore of the lake, contained only kaolinite and smectite. Illite, chlorite, kaolinite, and smectite were all present in suspended sediments from Tonle Sap Lake and surface sediments from the Tonle Sap River. Because illite and chlorite are not produced locally, they were assumed to be the products of weathering in the Mekong River basin, upstream of the Tonle Sap River. They are delivered to Tonle Sap Lake by the Tonle Sap River, and appeared in the lake sediment record only after Tonle Sap Lake and the Mekong River became connected.

In contrast to inferences from lithology and mineralogy, pollen assemblages in a Tonle Sap sediment core suggested that the lake and the Mekong were connected throughout the Holocene (Penny 2006).

The presence of *Rhizophora* (mangrove) pollen and *Thalassiosira bramaputrae* (Ehr.) Hak. & Lock., a brackish diatom, in the early Holocene portion of the sediment record indicated higher salinity in and around the lake at that time. Penny (2006) inferred that this higher salinity was indicative of a connection between Tonle Sap Lake and the South China Sea via the Mekong River. Thus, he concluded that the current hydrologic configuration of the Tonle Sap-Mekong system has existed throughout the Holocene. Penny (2006) attributed changes in pollen assemblages since ~5,000 years BP to an altered flooding regime induced by increased seasonality.

Materials and methods

We performed isotopic, XRF, C/N and P analysis, and radiocarbon dating on sediment cores from Tonle Sap Lake in order to constrain changes in sediment provenance, timing of flood pulse initiation, and ecology. In December 2003, two sediment cores were collected from Tonle Sap Lake (Fig. 1). Core TS-18-XII-03 is 5.85 m long and was retrieved from 4.28 m of water in the southeastern part of Tonle Sap Lake (12°36′11″N, 104°17′10″E). Core CHH-17-XII-03 is 6.25 m long and was taken from a water depth of 4.0 m in Tonle Chmaa, an open area on the northern edge of the main lake basin that is hydrologically connected to the lake, but separated by aquatic vegetation (12°49′31″N, 104°18′21″E) (Fig. 1). Thirteen cm of Core CHH-17-XII-03 between 5.25 and 5.12 m below lake floor (mblf) were lost on recovery. The elevation of the sediment surface of the core sites, and throughout most of the flat-bottomed lake basin, is approximately 0 m above sea level. Magnetic susceptibility in cores was measured at 0.5-cm intervals using a GEOTEK MultiSensor Core Logger. The cores were split lengthwise and imaged using a GEOTEK digital color line-scan camera.

The split cores were analyzed with an Avaatech XRF (x-ray fluorescence) core scanner at 1-cm resolution to provide close-interval elemental data. Measurements of elements Al to Ba were made using a slit size of 1 × 1 cm and generator settings of 10, 30, and 50 kV over 30 s of counting time. XRF core scanning is non-destructive, relatively rapid, and provides nearly continuous data (Tjallingii et al. 2007). Data from 1.13 to 1.05 mblf in core TS-18-XII-03 were considered unreliable because an uneven sediment surface caused by core splitting interfered with XRF measurements. Reduction of the XRF data set was accomplished by factor analysis using PASW Statistics 18.0. Three factors were extracted using principal components analysis with Varimax rotation. Small sections of the TS-18-XII-03 data set were excluded from the factor analysis, including an organic mud (5.54–4.94 mblf) and a *Corbicula* shell layer at 0.60–0.50 mblf. These distinctive beds dominated the factor analysis and were removed to reveal other trends in the data.

Sediment cores were sampled every 5–40 cm and samples were dried overnight at 60°C in an oven, and ground to a powder for geochemical analysis. Sr, Nd, and Pb were separated for radiogenic isotope analysis using standard chromatographic methods in a clean laboratory. Radiogenic isotope ratios were measured on a Nu-Plasma MC-ICP-MS using the protocol for highly precise measurements of small samples described by Kamenov et al. (2009). $^{87}Sr/^{86}Sr$ values were normalized to $^{86}Sr/^{88}Sr = 0.1194$ and ^{87}Sr was corrected for the presence of Rb by subtracting the counts of ^{87}Rb expected given an $^{87}Rb/^{85}Rb$ of 0.386. The long-term mean $^{87}Sr/^{86}Sr$ ratio of the standard NBS 987 is 0.710246 (±0.000030, 2σ). ^{144}Nd, ^{148}Nd, and ^{150}Nd were corrected for mass-bias from Sm using $^{147}Sm/^{144}Sm = 4.88$, $^{147}Sm/^{148}Sm = 1.33$, and $^{147}Sm/^{150}Sm = 2.03$. All measured ratios were normalized to $^{146}Nd/^{144}Nd = 0.7219$. The long-term mean $^{143}Nd/^{144}Nd$ of the standard JNdi-1 was 0.512107 (±0.000021, 2σ). Pb isotope compositions were measured using a Tl normalization technique (Kamenov et al. 2009). Pb data are relative to the following values of standard NBS 981: $^{206}Pb/^{204}Pb = 16.937$ (±0.004, 2σ), $^{207}Pb/^{204}Pb = 15.490$ (±0.003, 2σ), and $^{208}Pb/^{204}Pb = 36.695$ (±0.009, 2σ).

Weight percent C and N of bulk sediment were measured on a Carlo Erba NA1500 CNS Elemental Analyzer. C/N ratios are expressed as atom ratios. Stable C and N isotopes were measured on a Finnigan-MAT 252 or a Thermo Finnigan DeltaPlus XL isotope ratio mass spectrometer running in continuous flow mode. Analytical precision (one standard deviation) was ±0.09‰ for $\delta^{13}C$ and ±0.10‰ for $\delta^{15}N$. Samples analyzed for total P were digested in 5.0% H_2SO_4 and 5.0% K_2SO_8 in an autoclave and measured using a Bran-Luebbe Autoanalyzer (Kenney et al. 2001).

Radiocarbon dates were obtained on chemically pretreated wood, shell (*Corbicula* sp.), and decarbonated bulk sediment samples at the Center for Accelerator Mass Spectrometry (CAMS) at Lawrence Livermore National Laboratories and the NERC Radiocarbon Facility (Environment) and SUERC AMS Laboratory. Bulk sediment samples processed at CAMS were decarbonated using 1 N HCl with vortexing to prevent clumping, spun down, decanted and rinsed 3 times with Milli-Q water. The sediment was then dried overnight on a heating block and converted to CO_2 in individual quartz tubes using CuO as an oxygen source. Wood samples received a modified "de-Vries" chemical pretreatment and an acid–base-acid treatment at 90°C followed by copious rinsing with MQ water. Shells were cleaned of any adhering material, coarsely crushed, and leached in weak HCl before rinsing and drying on a heating block overnight. Carbonate was acid hydrolyzed in individual vacutainers following the methods described in Guilderson et al. (2003). Bulk sediment samples processed at the NERC Radiocarbon Facility (Environment) were digested in 2 M HCl at 80°C for 8 h, then washed with deionized water and dried and homogenized. Samples were converted to CO_2 by heating with CuO in sealed quartz tubes and the gas was converted to graphite by Fe/Zn reduction. Dates were calibrated to calendar years before present (cal year BP) using Calib html version 6.0 (Stuiver and Reimer 1993) that uses the IntCal09 radiocarbon calibration curve (Reimer et al. 2009) (ESM 2).

Results

Lithology

The stratigraphy of core TS-18-XII-03 is summarized in Fig. 2. The base of the core (unit I, 5.85–5.54 mblf) consists of a massive yellowish brown (10YR 5/4) mud that gradually grades into the overlying unit, consisting of very dark grayish brown (2.5Y 3/2) organic mud (unit II, 5.54–4.94 mblf). The third unit (4.94–0.90 mblf) is a massive olive (5Y 4/3) mud that has a sharp, wavy contact with the uppermost unit IV (0.90–0 mblf), consisting of a brown (10YR 4/3) mud that contains *Corbicula* sp. shells between 0.60 and 0.15 mblf. The greatest density of *Corbicula* shells occurs between 0.20–0.15 and 0.58–0.46 mblf.

The stratigraphy of core CHH-17-XII-03 is summarized in Fig. 3. The base of the core (unit I, 6.24–4.10 mblf) is a very dark, grayish brown (10YR 3/2) silty clay, intercalated with lenses of organic-rich sediment. This unit gradually grades into unit II (4.10–2.06 mblf), comprising a massive, dark grayish brown (2.5Y 4/2) silty clay. The contact between unit II and III (2.06–0.53 mblf) is diffuse, with unit III comprising a massive, olive (5Y 4/3) silty clay. A sharp contact marks the boundary between units III and IV (0.53–0 mblf), a brown (10YR 4/3) silty clay that contains *Corbicula* shells between 0.53 and 0.05 mblf. Unfortunately, a continuous section of core was cut into two sections at the contact between unit III and IV because this coincided with a joint between two coring tubes connected for a single drive. No material is missing at this contact, however.

Magnetic susceptibility and elemental abundances

Magnetic susceptibility in core TS-18-XII-03 increases nearly three-fold above 0.90 mblf (Fig. 4). Magnetic susceptibility in core CHH-17-XII-03 increases above 0.53 mblf (Fig. 5). C/N (atom) ratios are variable, but generally decrease upcore, with the lowest values in unit IV. Three factors account for 88.6% of the variance in the TS-18-XII-03 XRF data set (Fig. 6; ESM 3). Detrital elements Al, Si, Ti, and Zr load strongly on Factor 1, which accounts for 37.1% of the total variance. Factor 2 accounts for 35.5% of the variance and is dominated by alkali and alkali earth metals K, Rb, Ca, Sr, and Ba. Sixteen percent of the variance is explained by Factor 3 with loading scores dominated by the elements Fe and Mn. Factor 1 is relatively high below ~2.50 mblf, then decreases between 2.50 and 0.90 mblf. Above 0.90 mblf, Factor 1 abundances increase. Factor 2 shifts to higher values in the uppermost 0.90 m. Factor 3 also increases in unit IV, but exhibits several peaks between 3.00 and 2.00 mblf.

Geochemistry

All radiogenic isotopes measured in core TS-18-XII-03 changed above 0.90 mblf (Fig. 4). $^{87}Sr/^{86}Sr$ in unit I to III ranges from 0.71508 to 0.71930, although values below ~2.50 mblf (with the exception of unit II) are slightly less radiogenic than values between 2.50 and 0.90 mblf. In the uppermost 0.90 m, Sr values are between 0.71823 and 0.72169. ε_{Nd} values range from

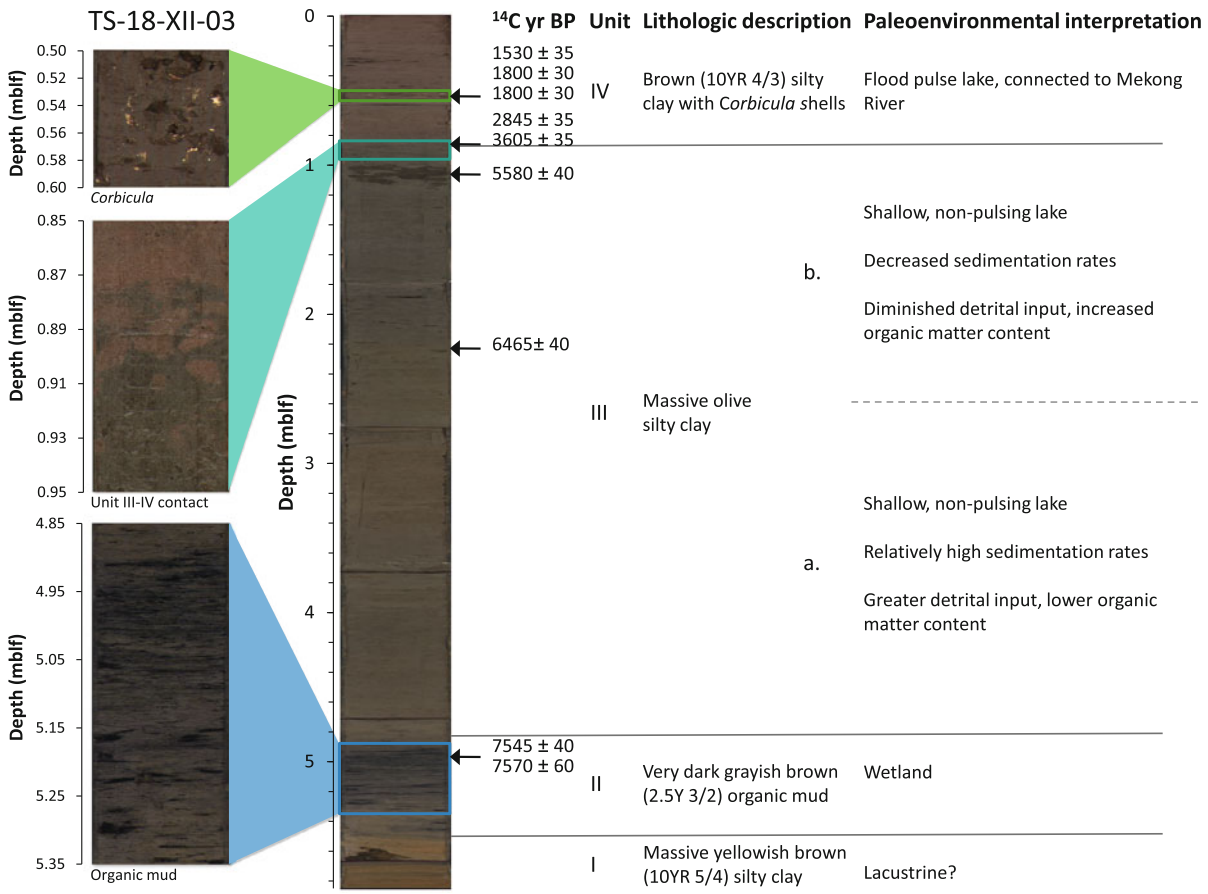

Fig. 2 Stratigraphy of core TS-18-XII-03. *Insets* of core photo show noteworthy features of the core in detail, including *Corbicula* shells, the uneven contact between units III and IV, and the organic-rich sediments in unit II. Radiocarbon dates are indicated

−6.1 to −7.6 in units I to III, while ε_{Nd} values in unit IV are between −8.2 and −9.8. $^{207}Pb/^{204}Pb$ values are between 15.657 and 15.669 below 0.90 mblf, and increase to between 15.673 and 15.689 above.

Weight %C and N in core TS-18-XII-03 are highest in unit II (Fig. 7). At ~2.50 mblf, weight %C increases slightly, then decreases above 0.90 mblf. Weight %N is variable overall, but increases above 2.50 mblf. C/N (atom) ratios peak in unit II and immediately above the unit III to IV transition, and decrease in the uppermost unit of the core (Fig. 7). Total P becomes more variable above 2.50 mblf, and P concentrations increase overall in unit IV. $\delta^{13}C_{bulk}$ values become more negative, while $\delta^{15}N_{bulk}$ values become more positive above 0.90 mblf (Fig. 7). Total P concentrations in core CHH-17-XII-03 are nearly constant in units I to III, then increase by an order of magnitude above 0.53 mblf (Fig. 5). $\delta^{15}N$ values decrease in units II and III, but increase to their most positive values in the uppermost unit of the core. $\delta^{13}C$ values become more negative above 0.53 mblf. Sediments from both Tonle Sap and Tonle Chmaa contain no carbonate material except for the *Corbicula* shells present in unit IV of both cores. Thus, weight %C and $\delta^{13}C$ values represent the organic C fraction.

Chronology

Radiocarbon dates from both cores are reported in ESM 2. At the two depths where wood was dated in core TS-18-XII-03, bulk sediment from the same depths was also dated to evaluate possible hard-water lake error (Deevey and Stuiver 1964). Age differences between these paired wood and sediment dates are 25 ^{14}C years (4.96–4.98 mblf) and 760 ^{14}C years (0.85–0.87 mblf) (ESM 2). Bulk sediment ages from

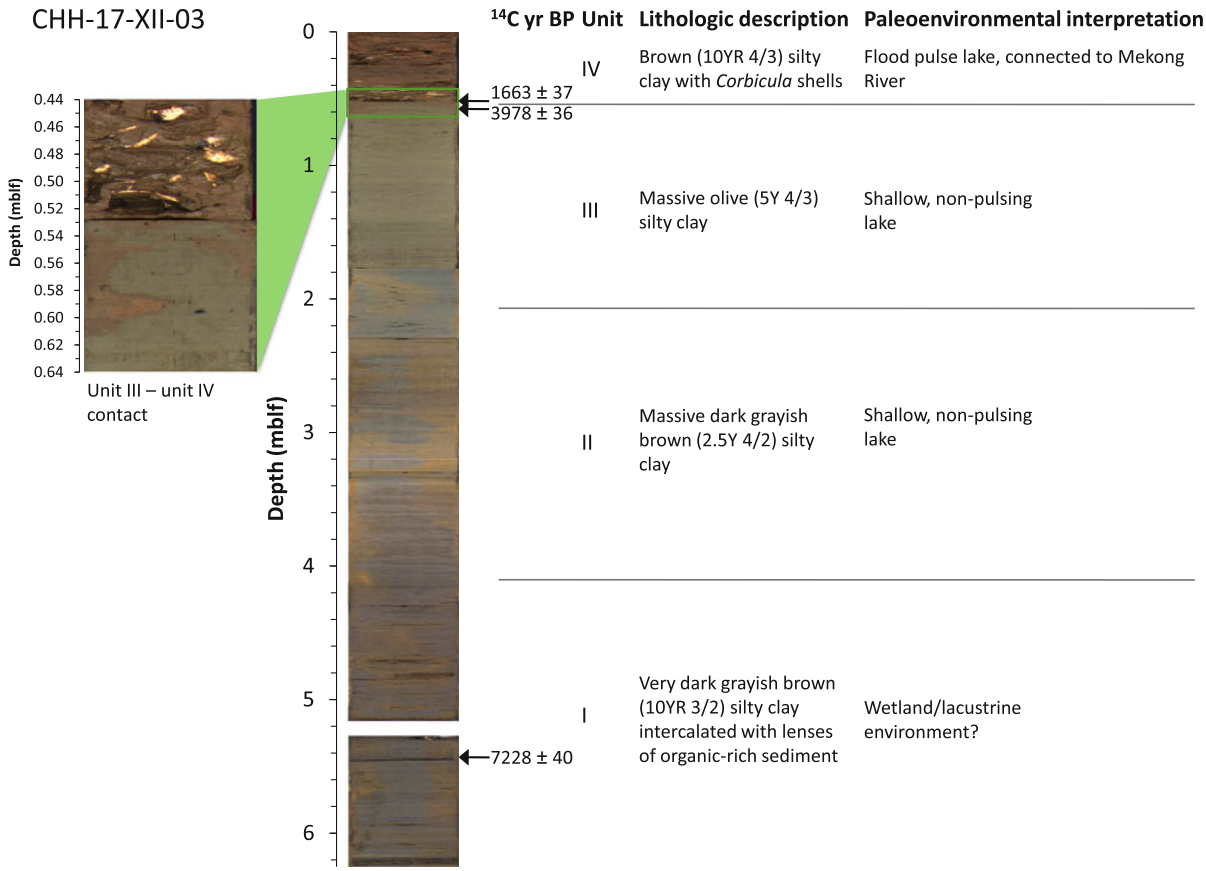

Fig. 3 Stratigraphy of core CHH-17-XII-03. Detail of core photo shows transition from units III to IV. The gap in the core photograph reflects the 13 cm of material lost on recovery. Radiocarbon dates are indicated

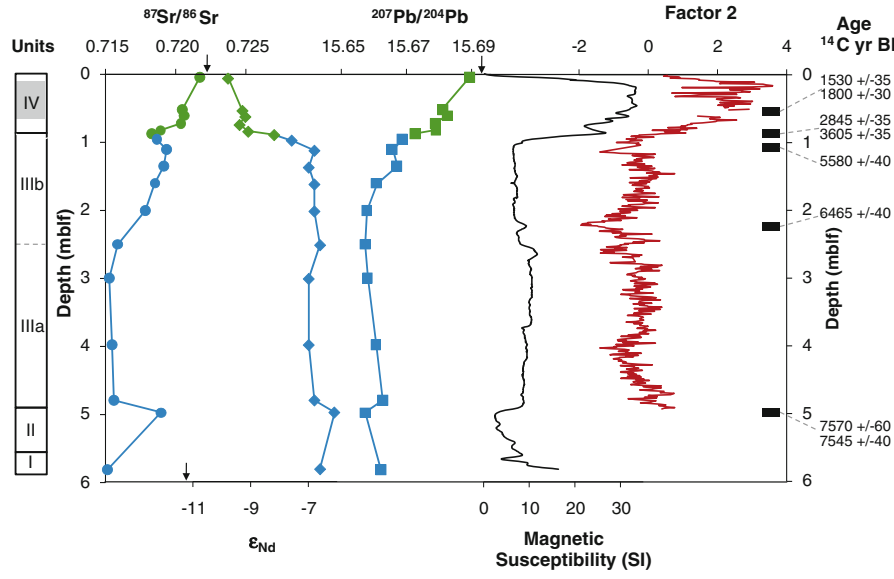

Fig. 4 $^{87}Sr/^{86}Sr$, ε_{Nd}, $^{207}Pb/^{204}Pb$, magnetic susceptibility, and Factor 2 from XRF data set for core TS-18-XII-03. *Arrows* on the *horizontal axes* of the $^{87}Sr/^{86}Sr$, ε_{Nd}, and $^{207}Pb/^{204}Pb$ curves indicate the mean published value for the Mekong River (see text for citations). Sediment units are indicated on the far *left*. *Shaded area* in unit IV represents *Corbicula* shell layer. Radiocarbon dates are indicated on the far *right*

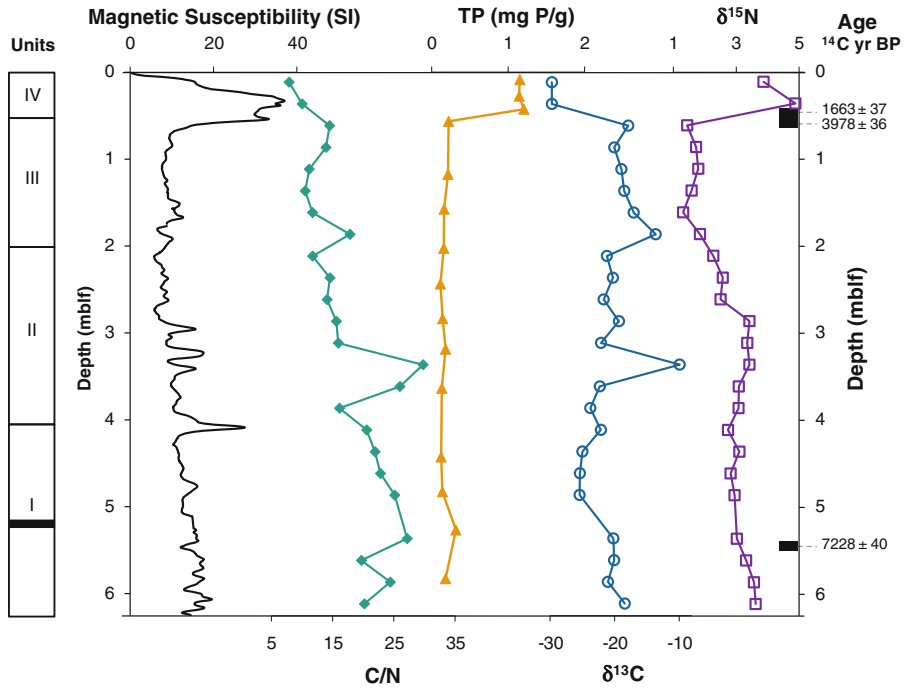

Fig. 5 Magnetic susceptibility, C/N (atom) ratio, total P (TP), δ^{13}C, and δ^{15}N for core CHH-17-XII-03. Sediment units are indicated on the far *left*. *Shaded portion* of unit I indicates portion of core lost on recovery. Radiocarbon dates are indicated on the far *right*

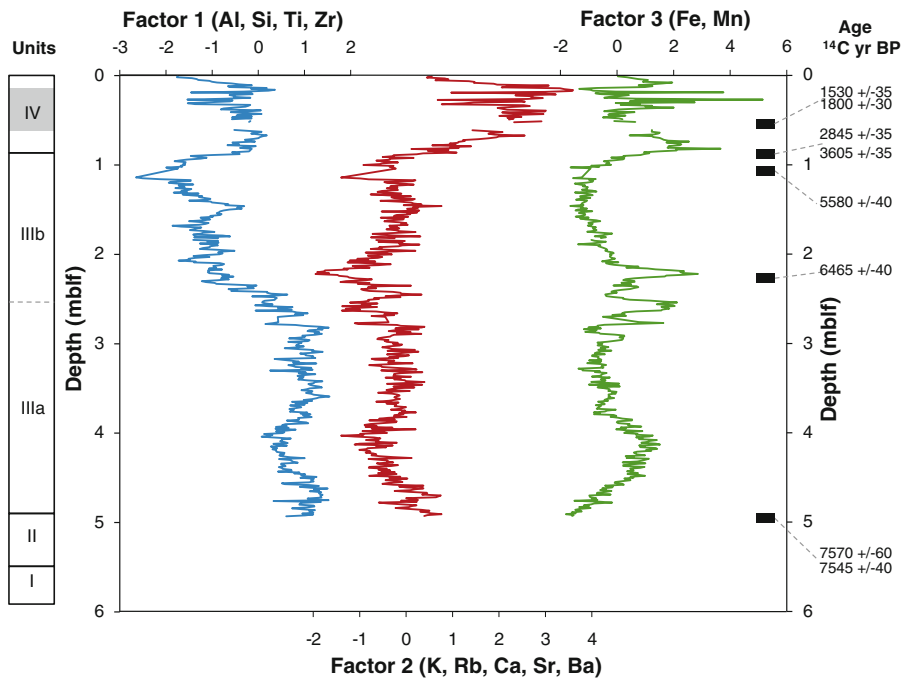

Fig. 6 Rotated factor solutions from factor analysis of scanning XRF data from core TS-18-XII-03. Elements represented by each factor are indicated. Sediment units are indicated on the far *left*. *Shaded area* in unit IV represents *Corbicula* shell layer. Radiocarbon dates are indicated on the far *right*

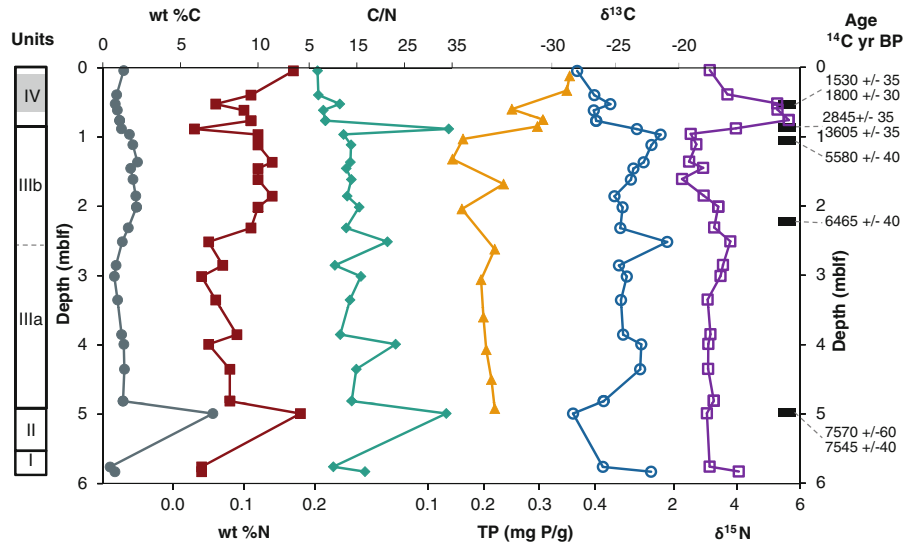

Fig. 7 Weight %C, weight %N, C/N (atom) ratio, total P (TP), $\delta^{13}C$, and $\delta^{15}N$ for core TS-18-XII-03. Sediment units are indicated on the far *left*. *Shaded area* in unit IV represents *Corbicula* shell layer. Radiocarbon dates are indicated on the far *right*

both cores are therefore considered to be reliable to at least 760 ^{14}C years. Mean sedimentation rate for core TS-18-CII-03, calculated by linear regression, changed from 2.0 mm year^{-1} below 0.90 mblf to 0.3 mm year^{-1} above (Fig. 8). Sedimentation rates for core CHH-17-XII-03 are similar, with 1.4 mm year^{-1} for unit I to III and 0.3 mm year^{-1} for unit IV. These values are consistent with previously published sedimentation rates for Tonle Sap Lake [modern lake: 0.3 mm ^{14}C year^{-1} (Carbonnel 1963); 7,532–5,460 cal year BP: 1.2 mm year^{-1}, between 2,035 and 610 cal year BP: 0.06 mm year^{-1} (Core S2C1) (calculated from Penny et al. 2005); 6,942–6,432 cal year BP: 1.1 mm year^{-1}, since 6,432 cal year BP: 0.08 mm year^{-1} (Core TS96-2) (calculated from Tsukawaki 1997)].

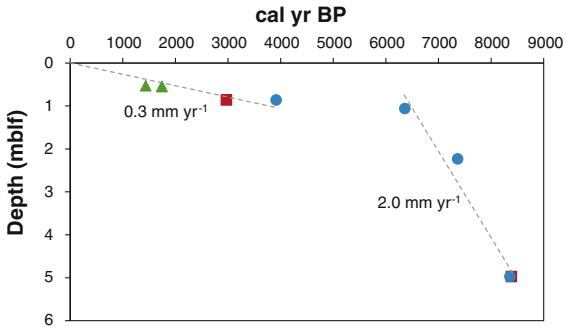

Fig. 8 Sedimentation rates for core TS-18-XII-03. Shell dates are indicated by *green triangles*, wood dates by *red squares*, and bulk sediment dates by *blue circles*

Discussion

Holocene transformations of Tonle Sap Lake

Changes in lithology, magnetic susceptibility, elemental abundances, radiogenic isotopes, stable isotopes, elemental ratios, and sedimentation rates indicate that each of the four sediment units in core TS-18-XII-03 represents a distinct period in the evolution of Tonle Sap Lake. The earliest Holocene is represented by unit I. Because few data were collected from this unit, detailed inference of the paleoenvironmental conditions it represents is not possible. The relatively low C/N ratios (Fig. 7), however, suggest an algal source of organic matter and thus a lacustrine environment. High C/N values and increased organic matter content in unit II suggest the presence of a vegetated wetland rather than a lake. The top of the second unit dates to approximately 8,200 cal year BP. The "8.2 kyr event," first recognized in the North Atlantic (Alley et al. 1997), has been identified as a dry period in several records from monsoon Asia (Fleitmann et al. 2007; Hong et al. 2005; Hu et al. 2008; Wang et al. 1999). Unit III marks the return to a lacustrine environment. The transition from unit II to unit III may also be related to sea level rise. Mekong Delta sediments indicate a period of rapid transgression around the 8.2 kyr event and this could have contributed to the shift from wetland to lacustrine conditions (Nguyen et al. 2010; Tamura et al. 2009).

Although unit III is lithologically relatively homogenous, conditions within Tonle Sap Lake changed around 6,500 ^{14}C year BP. Sedimentation rates decreased from 2.7 mm year^{-1} between ~4.94 and 2.50 mblf to 1.2 mm year^{-1} between ~2.50 and 0.90 mblf. Detrital input to Tonle Sap decreased between ~2.50 and 0.90 mblf as well, as reflected by the lower abundances of Al, Si, Ti, and Zr represented by Factor 1 (Fig. 6). Accordingly, the organic matter content of the sediments increased during this period. These changes could be the result of diminishing summer monsoon strength throughout the Holocene (Dykoski et al. 2005; Fleitmann et al. 2007). Reduced precipitation could result in less discharge and sediment transport to the lake from rivers within the Tonle Sap basin.

The abrupt transition from unit III to IV represents the change from a non-pulsing lake to the modern, Mekong River-connected, flood-pulsing Tonle Sap system. The shift in Sr, Nd, and ^{207}Pb/^{204}Pb isotopes in the uppermost unit represents a change in the provenance of sediments deposited in Tonle Sap Lake (Fig. 4). When compared to isotope values of Mekong River sediments (Liu et al. 2007; Millot et al. 2004; Schimanski et al. 2001) and marine sediments from the South China Sea derived largely from the Mekong (Liu et al. 2005), all values in the Tonle Sap core display a shift towards Mekong River sediment values beginning at 0.90 mblf (Fig. 9). All Mekong River sediment samples were collected near the mouth of the river, and thus provide an integrated radiogenic isotope signature for the entire Mekong basin. Given that the Tonle Sap River joins the Mekong quite close to the delta region, it is reasonable to assume that the isotopic signature for the entire basin approximates that of the sediments that enter Tonle Sap Lake via the Tonle Sap River. Marine sediments from the Vietnamese Shelf contain material from sources other than the Mekong, but the river provides most of the material to this region today (Liu et al. 2005). The isotope values from these marine sediments reflect the average isotopic signature of the Mekong-derived sediments that enter Tonle Sap Lake. Using total suspended solids (TSS) data, Kummu et al. (2008) concluded that 72% of the modern sediment deposited in Tonle Sap originates from the Mekong, whereas only 28% is derived from the lake's catchment. It was therefore expected that the bulk chemistry of Tonle Sap sediments would shift toward Mekong values once the "river–lake" connection was established. Sr and Nd isotope values from Mekong-derived sediments in a core from the South China Sea are similar over the last 140,000 years, indicating no change in the Mekong endmember ratios (Liu et al. 2005). Higher magnetic susceptibility in unit IV (Fig. 4) and the greater abundance of alkali and alkali earth metals indicated by Factor 2 (Fig. 6) are also attributed to input of Mekong sediments. Higher K abundances in the modern lake sediments are consistent with the results of Okawara and Tsukawaki (2002), who reported the presence of K-bearing illite in the lake sediments only above the observed lithologic boundary (correlative to unit III to IV transition in core TS-18-XII-03).

In the modern lake system, concentrations of TSS have been reported to vary with water level. TSS peak at the end of the dry season (April to June) when water levels are lowest (Campbell et al. 2006; Nagid et al. 2001; Sarkkula et al. 2004). TSS are consistently higher in the open lake than in the flooded forest because vegetation inhibits wind-driven resuspension of particles and traps sediment in the floodplain (Sarkkula et al. 2004). Persistent resuspension of sediment by wind and wave-induced currents in the modern lake means little material settles to be deposited permanently, as reflected in the low sedimentation rate (0.3 mm year^{-1}) in unit IV of both cores TS-18-XII-03 and CHH-17-XII-03. Instead, sediments are removed from the lake via the outflow and accumulate in the floodplain (MRCS/WUP-FIN 2003). The turbid nature of the lake, combined with dramatic fluctuations in water level, severely inhibits growth of submerged aquatic vegetation, despite the ubiquity of such plants throughout Southeast Asia (Campbell et al. 2006). Instead, algae and floating mats of herbaceous vegetation are common, as both of these primary producers outcompete submerged vegetation for light.

Ecological implications of the connection

When Tonle Sap Lake was a non-pulsing system (unit III), the ecology of the ancient lake would have been considerably different from the modern system. Changes in C/N ratios in the uppermost units of both cores reflect the transformation that occurred with the onset of the annual flood pulse (Figs. 5, 7). Lower

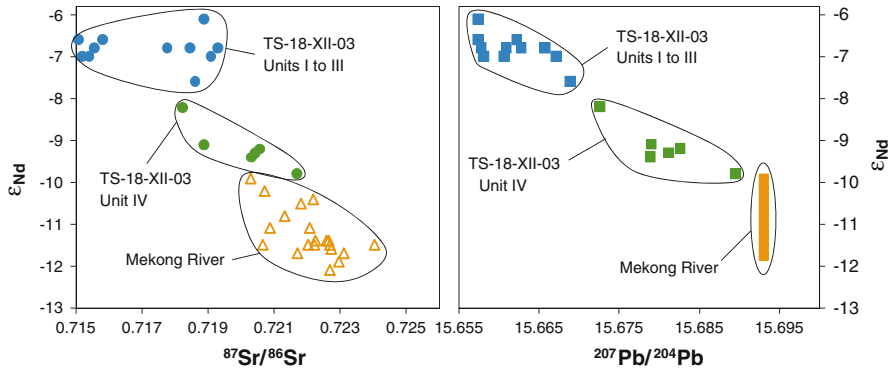

Fig. 9 ε_{Nd} values from core TS-18-XII-03 plotted against $^{87}Sr/^{86}Sr$ (*left*) and $^{207}Pb/^{204}Pb$ (*right*). Blue symbols denote lake sediments from units I to III (pre-connection). Green symbols denote lake sediments from unit IV (post-connection). *Yellow triangles* (*left*) are Mekong River values reported by Liu et al. (2005, 2007). *Yellow bar* (*right*) indicates range of ε_{Nd} values encountered in the literature (Liu et al. 2005, 2007; Schimanski et al. 2001) plotted against the only reported $^{207}Pb/^{204}Pb$ value (Millot et al. 2004)

C/N ratios in unit IV indicate greater relative input of organic matter from phytoplankton. An increase in the phytoplankton-derived contribution to sediment organic matter can likely be attributed to greater phytoplankton production within the lake. This result is consistent with predictions made by the flood pulse concept (Junk et al. 1989). Higher concentrations of total P in the uppermost unit of both cores, but especially CHH-17-XII-03, also suggest greater productivity since the initiation of the flood pulse. Exchange of nutrients between the permanently flooded lake and the floodplain promotes greater autochthonous organic matter production than would occur in a non-pulsing lake. Sediments brought into the lake with floodwaters may be another important source of nutrients, especially phosphorus (MRCS/WUP-FIN 2003). Floodplain processes, such as the decomposition of terrestrial vegetation, are likely a significant source of nutrients as well (Furch and Junk 1992, 1997). The rich Tonle Sap fishery provides evidence of great production. A fishery as productive as it is today likely could not exist without the "flood pulse advantage."

The decrease in $\delta^{13}C$ and increase in $\delta^{15}N$ in unit IV of both cores may reflect the intensification of organic matter exchange between the aquatic and terrestrial environments. As predicted by the FPC, greater quantities of terrestrially derived organic material become available to aquatic organisms during periods of flooding. Although lower C/N values indicate that sediment organic matter is aquatically produced, relatively negative $\delta^{13}C$ values and more positive $\delta^{15}N$ values reveal the terrestrial origin of organic material cycled through the Tonle Sap ecosystem.

Timing of flood pulse initiation

Radiocarbon dates 3 cm above and 15 cm below the contact between units III and IV in core TS-18-XII-03 indicate that the modern Tonle Sap Lake system developed between 5,580 ± 40 and 3,605 ± 35 to 2,845 ± 35 ^{14}C year BP. Due to the relative lack of organic terrestrial remains throughout the core for radiocarbon dating, as well as the likelihood of bioturbation over the unit III to IV contact (Fig. 2), it was difficult to obtain a more precise determination of the timing of the initial Tonle Sap-Mekong connection from this core. The timing of flood pulse initiation is better constrained by correlating cores TS-18-XII-03 and CHH-17-XII-03. The transition from units III to IV in both cores is marked by the same lithologic change and increase in magnetic susceptibility. Thus, unit IV represents the modern, flood pulse system in both cores. In core CHH-17-XII-03, the unit III to IV boundary is bracketed by radiocarbon dates of 3,978 ± 36 ^{14}C year BP and 1,663 ± 37 ^{14}C year BP, 2 cm below and 1 cm above the transition, respectively. Using two radiocarbon dates, one from each core, provides the best constraints on the timing of the unit III to IV boundary. Thus, the initiation of the Tonle Sap flood

pulse occurred between 3,978 ± 36 ^{14}C year BP and 3,605 ± 35 ^{14}C year BP (4,450 and 3,910 cal year BP). Given this revised timing, flood pulse initiation does not coincide with major changes in sea level, but rather seems to have occurred at a time of changing monsoon intensity (Cullen et al. 2000; Mayewski et al. 2004; Selvaraj et al. 2007; Staubwasser et al. 2003). Nonetheless, the processes responsible for initiating the flood pulse are related to the Mekong and one would not expect sediments from Tonle Sap Lake to record these changes.

Radiocarbon dates above and below the unit III to IV boundary are in agreement with published ^{14}C ages above and below the lithologic transition from other Tonle Sap cores. As with cores TS-18-XII-03 and CHH-17-XII-03, core correlation is based on changes in magnetic susceptibility and/or lithostratigraphy. ESM 1 summarizes the radiocarbon dates above and below the boundary in several cores from Tonle Sap Lake. Tsukawaki (1997) obtained an age of 5,081 ± 86 ^{14}C year BP across the lithologic transition in core TS96-1. For core TS96-2, Tsukawaki (1997) reported a date of 5,620 ± 120 ^{14}C year BP immediately below the transition. Penny et al. (2005) reported dates of 4,990 ± 40 ^{14}C year BP ~25 cm below the stratigraphic change in core S2C1 (marked by both a change in sediment color and an increase in magnetic susceptibility) and 2,070 ± 40 ^{14}C year BP ~30 cm above it. By dating material <5 cm above and below the lithologic transition (closer than previous studies), the radiocarbon dates from this study narrow the estimated age for the timing of flood pulse initiation.

Sedimentation in Tonle Sap Lake

Given the flat, shallow nature of the lake basin, Tonle Sap would have likely maintained a relatively stable, shallow depth year round during the deposition of unit III. Although local monsoon precipitation may have caused an increase in lake water level each rainy season, without input of floodwaters from the Mekong, the extreme changes in depth that occur in the lake today would not have occurred. Higher sedimentation rates (2.0 mm year^{-1}) in the non-pulsing Tonle Sap suggest that sediments accumulated permanently on the bottom of the lake much more so than today. The high relative abundance of the planktonic diatom *Aulacoseira* in the early Holocene portion of Penny's (2006) Tonle Sap record, suggests the lake was likely as turbulent and turbid in the past as in the modern system. The shallow depth and large fetch of Tonle Sap, even prior to the connection to the Mekong, would have promoted sediment resuspension and turbidity. Lower sedimentation rates in the modern lake can be attributed to the increased export of sediment from the system that occurs as the floodwaters recede. Although there were concerns that sedimentation was increasing in Tonle Sap and the lake was in danger of filling up, this notion has since been dispelled (Penny et al. 2005). Instead, the annual flood pulse acts to prevent basin in-fill.

Implications of climate and human-induced changes for Tonle Sap Lake

The Tonle Sap fishery faces several threats. Recent increase in human population has led to overfishing as well as deforestation of the flooded forests as needs for agricultural land and firewood intensified (Hortle et al. 2004). Further modifications to the Tonle Sap floodplain will alter the interaction between the aquatic and terrestrial environments during the flood pulse. Construction of dams on the Mekong River threatens to disrupt the natural hydrology of Tonle Sap. Of greatest concern is the Lancang Cascade, a series of eight dams being constructed in southern China. These dams will provide hydroelectric power to local residents, but might also stabilize water levels in the Lower Mekong Basin. Most (57%) of the water that enters the lake originates in the Mekong (Kummu et al. 2008). Consequently, water levels and flow in the river are the primary control on the Tonle Sap flood pulse. A shorter, smaller flood pulse will lead to habitat loss and reduced production within Tonle Sap Lake (Hortle et al. 2004). Reduced sediment transport will decrease the amount of nutrients delivered to Tonle Sap during the rainy season, further inhibiting productivity.

Climate variability and shifting monsoon intensity in the Mekong catchment will also likely affect the magnitude of the flood pulse. This paleolimnologic record provides a means to trace historically how the changing hydrologic regime affected the ecology of Tonle Sap Lake. Unit III may serve as an example of a future Tonle Sap in which the Mekong flood pulse is reduced or eliminated. The altered nature of

organic material deposited and the increase in total P concentrations since the onset of the flood pulse lake demonstrate that the ecosystem functioned differently prior to the establishment of the annual flood pulse. These findings are consistent with modeling results (Kummu and Sarkkula 2008) that suggest alteration of the flood pulse would negatively impact the Tonle Sap fishery.

Conclusions

Sr, Nd, and Pb isotopes, along with magnetic susceptibility and elemental abundances, were used to identify changes in sediment provenance in two sediment cores from Tonle Sap Lake. Radiocarbon dates from these two cores narrowly constrain the timing of initiation of the annual flood pulse to between 4,450 and 3,910 cal year BP. The inception of flood pulse processes produced significant changes in lake ecology. C/N and stable isotope values of bulk organic matter indicate greater production of autochthonous organic material, while higher total P concentrations suggest increased P loading in the modern lake system. The Tonle Sap flood pulse creates optimal conditions for fishery productivity by increasing habitat and food availability. Damming of the Mekong River and variations in monsoon strength will alter the Tonle Sap flood pulse and potentially impact the fishery.

Acknowledgments This work was supported, in part, by research funds provided by the Marion and Adolph Lichtstern Fund and the Neukom Family Distinguished Service Professorship held by ALK. Additional support to MBD was provided by the Gates Cambridge Trust and a University of Florida Alumni Fellowship. Radiocarbon analyses for core TS-18-XII-03 were performed under the auspices of the U.S. Department of Energy by Lawrence Livermore National Laboratory under contract DE-AC52-07NA27344. Radiocarbon analyses for core CHH-17-XII-03 were funded by NERC Radiocarbon Analysis Allocation Number 1452.1009. Many thanks to Simon Crowhurst, Gianna Browne and Jaime Escobar for their enthusiastic assistance in the lab. This work was completed under authorization from the Ministry of the Environment of the Kingdom of Cambodia and with permission of the Director of the APSARA Authority. We greatly appreciate logistical support provided by the Center for Khmer Studies, particularly former executive director Dr. Philippe Peycam. Thanks also to Laurent Holdener, Jake Janisa, Yi Sokpol, KotYi Ney, Meas Uon, Heng Poy, and Kun Ny for their help in the field. Finally, we would like to acknowledge two anonymous reviewers for their helpful comments on the manuscript.

References

Alley RB, Mayewski PA, Sowers T, Stuiver M, Taylor KC, Clark PU (1997) Holocene climatic instability: a prominent, widespread event 8200 yr ago. Geology 25:483–486

Baran E (2005) Cambodian inland fisheries: facts, figures and context. World Fish Center, Penang 49 pp

Bayley PB (1991) The flood pulse advantage and the restoration of river-floodplain systems. Regul River 6:75–86

Campbell IC, Poole C, Giesen W, Valbo-Jorgensen J (2006) Species diversity and ecology of Tonle Sap Great Lake, Cambodia. Aquat Sci 68:355–373

Carbonnel JP (1963) Vitesse d'accumulation des sédiments récents du Grand Lac du Cambodge, d'après le carbone 14. Corrélations stratigraphique et morphotectonique: C R Acad Sci 257:2514–2516

Carbonnel JP, Guiscafré J (1965) Grand Lac du Cambodge: Sedimentologie et hydrologie, 1962–1963. Muséum National d'Histoire Naturelle de Paris, Paris

Cullen HM, deMenocal PB, Hemming S, Hemming G, Brown FH, Guilderson T, Sirocko F (2000) Climate change and the collapse of the Akkadian empire: evidence from the deep sea. Geology 28:379–382

Deevey ES, Stuiver M (1964) Distribution of natural isotopes of carbon in Linsley Pond and other New England lakes. Limnol Oceanogr 9:1–11

Dykoski CA, Edwards RL, Cheng H, Yuan D, Cai Y, Zhang M, Lin Y, Qing J, An Z, Revenaugh J (2005) A high-resolution, absolutely-dated Holocene and deglacial Asian monsoon record from Dongge Cave, China. Earth Planet Sci Lett 233:71–86

Farr TG, Rosen PA, Caro E, Crippen R, Duren R, Hensley S, Kobrick M, Paller M, Rodriguez E, Roth L, Seal D, Shaffer S, Shimada J, Umland J, Werner M, Oskin M, Burbank D, Alsdorf D (2007) The Shuttle Radar Topography Mission, Rev Geophys 45. doi:10.1029/2005RG000183

Fleitmann D, Burns SJ, Mangini A, Mudelsee M, Kramers J, Villa I, Neff U, Al-Subbary AA, Buettner A, Hippler D, Matter A (2007) Holocene ITCZ and Indian monsoon dynamics recorded in stalagmites from Oman and Yemen (Socotra). Quat Sci Rev 26:170–188

Furch K, Junk WJ (1992) Nutrient dynamics of submersed decomposing Amazonian herbaceous plant species *Paspalum fasciculatum* and *Echinochloa polystachya*. Rev Hydrobiol Trop 25:75–85

Furch K, Junk WJ (1997) Physicochemical conditions in the floodplains. In: Junk WJ (ed) Ecological studies, volume 126, The Central Amazon Floodplain: ecology of a pulsing system. Springer, New York, pp 69–108

Guilderson TP, Southon JR, Brown TA (2003) High-precision AMS ^{14}C results on TIRI/FIRI turbidite. Radiocarbon 45:75–80

Hong YT, Hong B, Lin QH, Shibata Y, Hirota M, Zhu YX, Leng XT, Wang Y, Wang H, Yi L (2005) Inverse phase oscillations between the East Asian and Indian Ocean summer monsoons during the last 12 000 years and paleo-El Niño. Earth Planet Sci Lett 231:337–346

Hortle KG, Lieng S, Valbo-Jorgensen J (2004) An introduction to Cambodia's inland fisheries. Mekong development series No. 4. Mekong River Commission, Phnom Penh

Hu C, Henderson GM, Huang J, Xie S, Sun Y, Johnson KR (2008) Quantification of Holocene Asian monsoon rainfall from spatially separated cave records. Earth Planet Sci Lett 266:221–232

Junk WJ, Wantzen KM (2004) The flood pulse concept: new aspects, approaches and applications—an update. In: Welcomme RL, Petr T (eds) Proceedings of the second international symposium on the management of large rivers for fisheries. RAP Publication, Bangkok, pp 117–140

Junk WJ, Bayley PB, Sparks RE (1989) The flood pulse concept in river-floodplain systems. In: Dodge DP (ed) Proceedings of the international large river symposium. Canadian Special Publication of Fisheries and Aquatic Science 106:110–127

Kamenov GD, Brenner M, Tucker JL (2009) Anthropogenic vs natural control on trace element and Sr-Nd-Pb isotope record in peat sediments of southeast Florida, USA. Geochim Cosmochim Acta 73:3549–3567

Kenney WF, Schelske CL, Chapman AD (2001) Changes in polyphosphate sedimentation: a response to excessive phosphorus enrichment in a hypereutrophic lake. Can J Fish Aquat Sci 58:879–887

Keskinen M, Koponen J, Kummu M, Nikula J, Sarkkula J, Varis O (2005) Integration of socio-economic and hydrological information in the Tonle Sap Lake, Cambodia. In: Proceedings, international conference on simulation and modeling, Bangkok

Kummu M, Sarkkula J (2008) Impact of the Mekong River flow alteration on the Tonle Sap flood pulse. Ambio 37:185–192

Kummu M, Penny D, Sarkkula J, Koponen J (2008) Sediment: curse or blessing for Tonle Sap Lake? Ambio 37:158–163

Lamberts D (2001) Tonle Sap fisheries: a case study on floodplain gillnet fisheries. Asia-Pacific Fishery Commission, Food and Agriculture Organization of the United Nations, Bangkok, Thailand, 101 pp

Lamberts D (2008) Little impact, much damage: The consequences of Mekong River flow alterations for the Tonle Sap ecosystem. In: Kummu M, Keskinen M, Varis O (eds) Modern myths of the Mekong. Water & Development Publications—Helsinki University of Technology, Helsinki, pp 3–18

Lamberts D, Koponen J (2008) Flood pulse alterations and productivity of the Tonle Sap ecosystem: a model for impact assessment. Ambio 37:178–184

Liu Z, Colin C, Trentesaux A, Siani G, Frank N, Blamart D, Farid S (2005) Late Quaternary climatic control on erosion and weathering in the eastern Tibetan Plateau and the Mekong Basin. Quat Res 63:316–328

Liu Z, Colin C, Huang W, Phon Le K, Tong S, Chen Z, Trentesaux A (2007) Climatic and tectonic controls on weathering in South China and Indochina Peninsula: clay mineralogical and geochemical investigations from the Pearl, Red, and Mekong drainage basins. Geochem Geophys Geosyst 8. doi:10.1029/2006GC001490

Mayewski PA, Rohling EE, Stager JC, Karlén W, Maasch KA, Meeker LD, Meyerson EA, Gasse F, van Kreveld S, Holmgren K, Lee-Thorp J, Rosqvist G, Rack F, Staubwasser M, Schneider RR, Steig EJ (2004) Holocene climate variability. Quat Res 62:243–255

Millot R, Allègre C-J, Gaillardet J, Roy S (2004) Lead isotopic systematics of major river sediments: a new estimate of the Pb isotopic composition of the Upper Continental Crust. Chem Geol 203:75–90

MRCS/WUP-FIN (2003) Modelling Tonle Sap for environmental impact assessment and management support: Water Utilization Program—modelling of the flow regime and water quality of the Tonle Sap. Finnish Environmental Institute Helsinki, Finland, 110 pp

Nagid EJ, Canfield DE, Hoyer MV (2001) Wind-induced increases in trophic state characteristics of a large (27 km^2), shallow (1.5 m mean depth) Florida lake. Hydrobiologia 455:97–110

Nguyen VL, Ta TKO, Saito Y (2010) Early Holocene initiation of the Mekong River delta, Vietnam, and the response to Holocene sea-level changes detected from DT1 core analyses. Sediment Geol 230:146–155

Okawara M, Tsukawaki S (2002) Composition and provenance of clay minerals in the northern part of Lake Tonle Sap, Cambodia. J Geogr (Chigaku Zasshi) 111:341–359

Penny D (2006) The Holocene history and development of the Tonle Sap, Cambodia. Quat Sci Rev 25:310–322

Penny D, Cook G, Im SS (2005) Long-term rates of sediment accumulation in the Tonle Sap, Cambodia: a threat to ecosystem health? J Paleolimnol 33:95–103

Reimer PJ, Baillie MGL, Bard E, Bayliss A, Beck JW, Blackwell PG, Bronk Ramsey C, Buck CE, Burr GS, Edwards RL, Friedrich M, Grootes PM, Guilderson TP, Hajdas I, Heaton TJ, Hogg AG, Hughen KA, Kaiser KF, Kromer B, McCormac FG, Manning SW, Reimer RW, Richards DA, Southon JR, Talamo S, Turney CSM, van der Plicht J, Weyhenmeyer CE (2009) IntCal09 and Marine09 radiocarbon age calibration curves, 0–50, 000 years cal BP. Radiocarbon 51:1111–1150

Ryan WBF, Carbotte SM, Coplan JO, O'Hara S, Melkonian A, Arko R, Weissel RA, Ferrini V, Goodwillie A, Nitsche F, Bonczkowski J, Zemsky R (2009) Global multi-resolution topography synthesis. Geochem Geophys Geosyst 10. doi:10.1029/2008GC002332

Sarkkula J, Baran E, Chheng P, Keskinen M, Koponen J, Kummu M (2004) Tonle Sap Pulsing System and fisheries productivity. Contribution to the XXIXe International Congress of Limnology (SIL 2004), Lahti, Finland

Schimanski A, Haase K, Stattegger K, Grootes PM (2001) Provenance of Holocene and recent sediments on the Vietnamese Shelf revealed by Sr and Nd isotopes and trace elements [abs.]. Eos (Transactions, American Geophysical Union), 82:OS42SA-0453

Selvaraj K, Chen CTA, Lou J-Y (2007) Holocene East Asian monsoon variability: links to solar and tropical Pacific forcing. Geophys Res Lett 34. doi:10.1029/2006GL028155

Staubwasser M, Sirocko F, Grootes PM, Segl M (2003) Climate change at the 4.2 ka BP termination of the Indus valley civilization and Holocene south Asian monsoon variability. Geophys Res Lett 30. doi:10.1029/2002GL016822

Stuiver M, Reimer PJ (1993) Extended ^{14}C database and revised CALIB radiocarbon calibration program. Radiocarbon 35:215–230

Tamura T, Saito Y, Sieng S, Ben B, Kong M, Sim I, Choup S, Akiba F (2009) Initiation of the Mekong River delta at

8 ka: evidence from the sedimentary succession in the Cambodian lowland. Quat Sci Rev 28:327–344

Tjallingii R, Röhl U, Kölling M, Bickert T (2007) Influence of the water content on X-ray fluorescence core-scanning measurements in soft marine sediments. Geochem Geophys Geosyst 8. doi:10.1029/2006GC001393

Tsukawaki S (1997) Lithological features of cored sediments from the northern part of Lake Tonle Sap, Cambodia. In: Dheeradilok P, Hinthong C, Chaodumrong P, Putthapiban P, Tansathien W, Utha-aroon C, Sattyarak N, Nuchanong T, Techawan S (eds) Proceedings of the international conference on stratigraphy and tectonic evolution of Southeast Asia and the South Pacific. Dept Min Res. Bangkok, Thailand, pp 232–239

Wang L, Sarnthein M, Erlenkeuser H, Grootes PM, Grimalt JO, Pelejero C, Linck G (1999) Holocene variations in Asian monsoon moisture: a bidecadal sediment record from the South China Sea. Geophys Res Lett 26:2889–2892

Wantzen KM, Junk WJ, Rothhaupt K-O (2008) An extension of the floodpulse concept (FPC) for lakes. Hydrobiologia 613:151–170